Correspondence and requests for materials should be addressed to G.-P.S. (gpsheng@ustc.edu.cn)

* These authors contributed equally to this work.

Experimental and Theoretical Approaches for the Surface Interaction between Copper and Activated Sludge Microorganisms at Molecular Scale

Hong-Wei Luo[1]*, Jie-Jie Chen[1]*, Guo-Ping Sheng[1], Ji-Hu Su[2], Shi-Qiang Wei[3] & Han-Qing Yu[1]

[1]CAS Key Laboratory of Urban Pollutant Conversion, Department of Chemistry, [2]Department of Modern Physics, University of Science and Technology of China, Hefei, 230026, China, [3]National Synchrotron Radiation Laboratory, University of Science and Technology of China, Hefei, 230029, China.

Interactions between metals and activated sludge microorganisms substantially affect the speciation, immobilization, transport, and bioavailability of trace heavy metals in biological wastewater treatment plants. In this study, the interaction of Cu(II), a typical heavy metal, onto activated sludge microorganisms was studied in-depth using a multi-technique approach. The complexing structure of Cu(II) on microbial surface was revealed by X-ray absorption fine structure (XAFS) and electron paramagnetic resonance (EPR) analysis. EPR spectra indicated that Cu(II) was held in inner-sphere surface complexes of octahedral coordination with tetragonal distortion of axial elongation. XAFS analysis further suggested that the surface complexation between Cu(II) and microbial cells was the distorted inner-sphere coordinated octahedra containing four short equatorial bonds and two elongated axial bonds. To further validate the results obtained from the XAFS and EPR analysis, density functional theory calculations were carried out to explore the structural geometry of the Cu complexes. These results are useful to better understand the speciation, immobilization, transport, and bioavailability of metals in biological wastewater treatment plants.

Interactions between metals and microorganisms play an important role in the geochemical cycling of trace heavy metals. In biological wastewater treatment processes, microorganisms in activated sludge have a high metal complexation capacity and then substantially affect the speciation, immobilization, transport, and bioavailability of metals in biological wastewater treatment plants. Previous study showed that there are many heavy metals (e.g., copper) in municipal and industrial wastewaters[1]. It is of great significance to study the surface complexation of metals on microorganisms and to understand their fates in biological wastewater treatment plants. In addition, extracellular polymeric substances (EPS), high-molecular weight compounds secreted by microorganisms, also have a significant impact on the fates of heavy metals[2,3]. The relevant functional groups involved in the interaction between metals and microorganisms are reported to be $-COOH$, $-OH$, $-NH_2$, and $-PO_4$, etc[4].

However, there are contradictory reports about the interaction between heavy metals and microbial cells in the presence and absence of EPS. In some studies it was found that the presence of EPS did not significantly affect the interaction[5]; while others reported that the presence of EPS had a substantial effect on the interaction[6]. Such a contradiction may be attributed to the different experimental techniques employed in these works. Furthermore, the complicated structures of activated sludge and high water content make it difficult to explore the interaction mechanisms between heavy metals and microbial cells at a microscale. Previous studies showed that activated sludge microorganisms had high complexing capability to Cu[7–9], which was particle-diffusion-controlled, and followed the pseudo-second-order rate kinetics[7]. The complexing process was also obeyed Freundlich and Langmuir models, and the saturation amount of Cu(II) adsorbed by biomass was found to be 2.00 mmol/g[9]. Although the macroscopic adsorption of many kinds of heavy metals (including Cu) onto activated sludge has been investigated intensively, and many analytical methodologies, such as potentiometric titrations, electrophoretic measurements, and infrared spectroscopy[10], have been also developed to characterize this interaction. However, the surface complexing microstructure between the heavy metals and the functional groups in the

sludge surface are still not well known. So there is still a need for further investigations of the surface interaction at molecular scale.

The main objective of this study is to get a deep insight into the microscopic-level interaction between heavy metal Cu(II) and activated sludge as well as its EPS, providing the microstructure of Cu(II) complexing with the functional groups of activated sludge. Spectroscopic measurements can be used to probe surface speciation and sorption mechanisms at molecular scale. For example, electron paramagnetic resonance (EPR) is able to give the geometrical information about paramagnetic metallic cations (e.g., Cu), and qualitative and quantitative information about unpaired electrons of heavy metals after complexation. X-ray absorption fine structure (XAFS) analysis is another important means to describe the local structure including bond distance, coordination number, and type of near-neighbors surrounding a specific element[11,12], which is very sensitive to molecular complexation. The density functional theory (DFT) calculation provides useful information about the interpretation of experimental spectroscopic data to identify possible coordination environments of adsorbed Cu[13-15]. The experimental and calculation results could provide more detailed microscopic chemical structure information about the interactions between heavy metals and activated sludge microorganisms, and thus would give a more crucial understanding in the fate of heavy metals in biological wastewater treatment plants.

Results and Discussion

Potentiometric titration curve and surface functional groups of activated sludge. The titration curve of pH *vs.* NaOH additions is

shown in Fig. 1a, and the corresponding derivative of the titration curve is illustrated in Fig. 1b. The activated sludge showed a certain buffering capacity, as indicated by the weak inflection points (Fig. 1a). The derivative of the titration curve (Fig. 1b) gave the equivalence points and the apparent pK_a values for the activated sludge. The peaks indicated a maximum variation in pH corresponding to the equivalence points, and the valleys showed a minimum variation in pH, which was an indicator of buffering. Arrows (at pHs of 5.8 and 8.3) represented the corresponding pH values of the titration curve for each equivalence points (Eq.$_n$)[16]. Assuming four binding sites according to the derivative of the titration curve, the pK_a values of the proton-binding sites as well as their contents were estimated using the PROTOFIT 2.1 software, and are shown in Fig. 1c. The pK_a values and their contents of the four binding sites were pK_{a1} 3.57 (0.25 mmol/g), pK_{a2} 5.42 (0.66 mmol/g), pK_{a3} 7.28 (0.37 mmol/g), and pK_{a4} 9.92 (1.12 mmol/g), which were assigned as phosphodiester, carboxyl, phosphoryl and hydroxyl/phenolic groups, respectively[17-19].

EPR results. The structural characteristics of the Cu(II)-activated sludge complexes were explored using EPR spectroscopy. The EPR spectra displayed an inconspicuous anisotropic copper signal both at 40 K and 298 K (Fig. 2), Theoretically Cu(II) standard should be a typical anisotropic signal with four lines ($2I + 1 = 4$) in parallel region arising from the hyperfine coupling of the $S = 1/2$ electron spin of Cu(II) with its nuclear spin $I = 3/2$. This suggests that the process of cooling had no obvious impact on the structural fate of the Cu(II) complexing, and the structure of Cu(II) complex was different
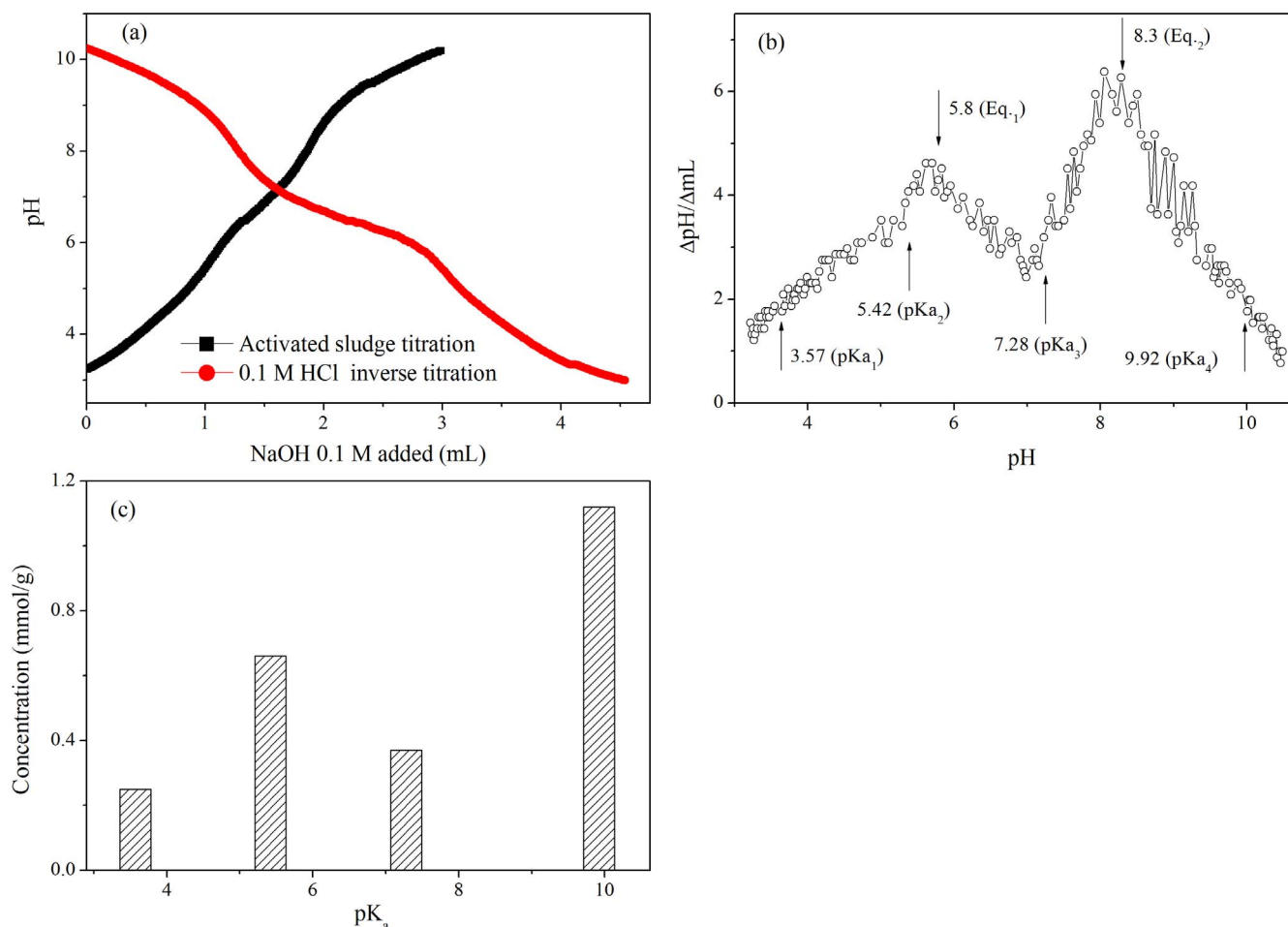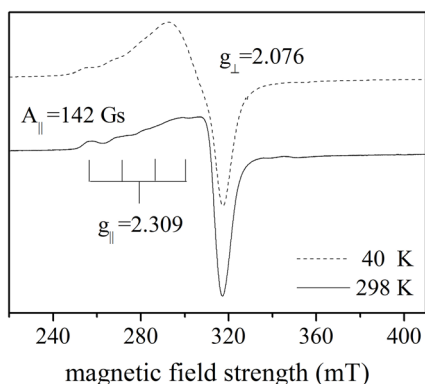

Figure 1 | Acid-base titration curve of activated sludge: (a) the corresponding derivative of the titration curve; (b) pK_a values of various binding sites; and (c) the corresponding concentrations of functional groups at various pKa values.

Figure 2 | EPR spectra of the Cu(II)- activated sludge complex at 298 K and 40 K.

with that of Cu(II) standard. EPR spectra reveal that the Cu(II) center was axial ($g_{\parallel} > g_{\perp} > g_e = 2.00$), with simulated spin Hamiltonian parameters $g_{\parallel} = 2.309$, $g_{\perp} = 2.076$, $A_{\parallel} = 142$ Gs (Fig. 2). The value of hyperfine coupling constant A for Cu(II) was a mean value corresponding to the ^{63}Cu and ^{65}Cu isotopes with their natural abundance. The fact $g_{\parallel} > g_{\perp} > g_e$ indicates that the copper ions had an octahedral coordination with tetragonal distortion of axial elongation (D4h symmetry) due to Jahn-Teller effect[20]. These values were consistent with a $d_{x^2-y^2}$ ground state for the Cu(II), and the parameter was in the range between those of the cation $Cu(H_2O)_6^{2+}$ ($g_{\parallel} = 2.440$) and those of $Cu(OH)_2$ ($g_{\parallel} = 2.267$). The $d_{x^2-y^2}$ orbital would increase the destabilization if an axial coordination around Cu(II) ion exists, which causes an increase in the g value from the following modified equations[21]:

$$g_z = g_{\parallel} = g_e + \frac{8|\lambda|}{\Delta E(x^2-y^2 \to xy)} \quad (1)$$

$$g_x = g_y = g_{\perp} = g_e + \frac{2|\lambda|}{\Delta E(x^2-y^2 \to xz,yz)} \quad (2)$$

where λ represents the spin-orbit coupling constant, ΔE is the difference in the corresponding state energies, and g_e is the g factor of the free electron. Here, $|\lambda| = 830$ cm^{-1} for Cu, $g_e = 2.0023$, thus ΔE can be calculated according to the measured g value, which is used for screening axially symmetric structure in the DFT calculations.

The surface complexation of Cu(II) ion decreased the $g_{\parallel}$-value compared with the value of the free Cu^{2+} ($Cu(H_2O)_6^{2+}$, $g_{\parallel} = 2.440$). The decrease in $g_{\parallel}$ could be associated with the total thermodynamic stability of the formed complex (K_{total}), as shown in eq 3[21]:

$$\log K_{total} = 84(2.44 - g_{\parallel}) \quad (3)$$

where 2.44 is the $g_{\parallel}$ value of the frozen solution aquo ion Cu^{2+}, which has been chosen as a reference point ($\log K_{total} = 0$).

From the relationship between the thermodynamic stability constants of surface complexes and the EPR parameter, the magnitude of Cu(II) complexing strength with the activated sludge could be estimated. The $g_{\parallel}$ value was measured to be 2.309, and thus the surface complex constant ($\log K_{total}$) was estimated to be 11.0, which was comparable to those between Cu and other ligands (e.g., montmorillonite, soil particles, humic substances) with plenty of various functional groups[22], implying the complexing mechanisms between Cu and these ligands might be the same.

XAFS analysis. The K-edge X-ray absorption spectra of Cu(II) complexing with the activated sludge before and after EPS extraction at various pH values were collected. The Cu K-edge

XANES spectra of samples and various standards are shown in Fig. 3. The pre-edge peak at 8976 eV (Arrow 1) was assigned to the 1s to 3d dipole-forbidden electronic transition (probably hybridized by p orbitals of the ligands)[23]. Another peak at 8981 eV (Arrow 2) was resulted from reduced Cu(I) signal. However, the presence of a shoulder at 8981 eV in the Cu absorption edge spectra and the absence of a pre-edge from 8976 eV indicate the presence of Cu(I) in the samples. This peak showed a slightly increase after sequential scans, suggesting a radiation-induced reduction of Cu(II)[24]. The other two peaks in the Cu K-edge XANES spectra (Arrows 3 and 4) were attributed to the 1s to 4p main edge electron transitions. The splitting of the derivative XANES spectra might result from anisotropic square planar symmetry of Cu(II) compounds, or could be referred to the tetragonal distortion of the CuO_6 octahedron due to Jahn-Teller effect. These inflections provided information about the three dimensional geometry and coordination environment of Cu in the Cu complexes. The Peak 3 and Peak 4 corresponded respectively to the 1s $\to$ 4p and 1s $\to$ continuum transitions for Cu(II) compounds in octahedral symmetry[25,26]. The energy gap between the two peaks was 5.0 eV (Fig. 3), attributed to the distortion of 4p$_z$ orbit in metalic center. This obtained value was of a similar level to those for other Cu(II) compounds in slightly tetragonally distorted octahedral environments, and was also in accordance with the EPR analytical results. Moreover, the sample spectra in our work had a distinct shoulder peak, which might be due to the degree of axial distortion and the covalence of the equatorial ligands bonded to Cu(II).

After the EPS were extracted from the activated sludge, the XANES spectra of the complexes between Cu and EPS-free activated sludge were shifted to the high energy side because of the increase in oxidation state from the complexes. Also, this phenomenon was observed when pH was increased from 3.0 to 7.0. This might be because the uncomplexed Cu(II) in the equilibrium solution became gradually precipitated to $Cu(OH)_2$, which increased the Cu content in the complex for the XAFS analysis. The extraction of EPS influenced the complexation ability of metal ions on the sludge[10], but no significant difference on the binding parameters of the Cu complexes, e.g., bond length and coordination number, was observed. The reason might be that the main functional groups in activated sludge with or without EPS would be similar, although their contents could be changed after the EPS extraction. Thus, the complexing structure between Cu(II) and sludge microorganisms after EPS extraction would not be influenced.
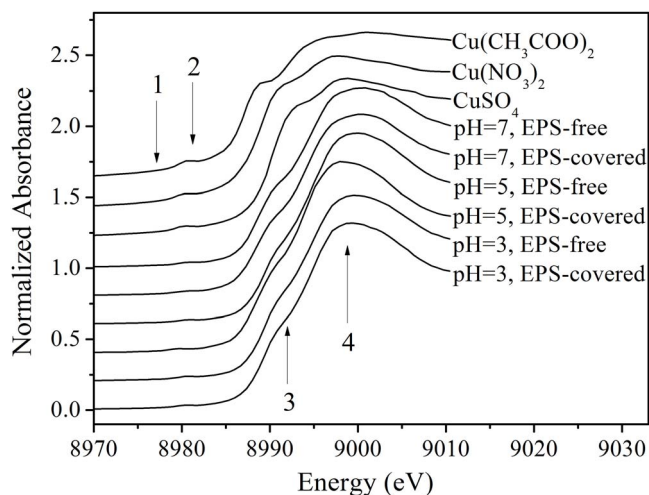

Figure 3 | X-ray absorption near-edge structure of reference compounds and Cu- activated sludge under different conditions.

To gain more insight into the molecular structure of the Cu complexing with activated sludge, the EXAFS spectra were fitted according to the standard model of $Cu(NO_3)_2$. The first-shell fit of the EXAFS spectra of the Cu complexes and its corresponding radial structure function (RSF) derived from Fourier transformations, are illustrated in Fig. 4. The position of the peaks in the RSF corresponds to the relative distance (uncorrected for phase shift) between Cu(II) and complexing atoms in local coordination shells. The strongest peak, which appears between 1.44 and 1.50 Å in Fig. 4a, corresponded to the first-shell O atoms. Within the framework of the single scattering approach, the EXAFS spectra fitted well by Levenberg-Marquardt fitting (Fig. 4b), and the results are listed in Table 1. The results show that Cu(II) ions were surrounded by four equatorial oxygen atoms and two axial oxygen atoms. The average $Cu\text{-}O_{eq}$ bond length was 1.95 ± 0.01 Å, and the $Cu\text{-}O_{ax}$ one was equal to 2.43 ± 0.50 Å. These data are consistent with those obtained from the EPR results and the XANES spectra: distorted octahedra containing four short equatorial bonds and two elongated axial bonds. Also, this agrees with previous studies, in which bond distance for $Cu\text{-}O_{eq}$ first shell has been reported to range from 1.92 to 1.97 Å[27–29], while the second shell Cu–O/C ranged from 2.29 to 2.41 Å[30].

As shown in Table 1, the fitting results of the second shell were more susceptible by the extraction of EPS and change of pH than those of the first shell. Because there were usually more coordinated atoms such as C, H and O associated with the complexation of the second shell, which would be influenced by the solution pH and sludge EPS. The bond lengths were in the range of 2.40–2.50 Å

and the coordination numbers varied from 1.5 to 1.8 in the second shell. However, the bond lengths were in a range of 1.93–1.95 Å, when the coordination numbers were kept at 4.0 for the first shell. Those bond lengths were in agreement with the reported values of Cu-hydroxyl or Cu-carboxyl from previous literatures[27–30]. From the microscopic view point, the observed fitting results of Cu(II) K-edge XAFS analysis was not significantly affected after EPS extraction on the bond lengths and coordination numbers. Thus in the short range of a few angstroms surrounded by Cu(II), the bond lengths and coordination numbers were able to stabilize regarding to the complexing structure of Cu and activated sludge microorganisms.

DFT calculation. To further support our interpretation based on EPR and XAFS, the proposed structures of Cu complex were studied by DFT calculations. The Cu(II) center stably existed in a 6-oxygen coordinated octahedron in EPS. The molecular orbital contour plot for the Cu complex and the splitting of energy levels are shown in Fig. S1. Cu 3d orbitals coordinate with π^*, σ orbitals from ligands, and the molecular orbital of Cu complex was split into t_{2g} and e_g^* with the splitting energy ~6000 cm^{-1}, corresponding to the energy $\Delta E = 4071\sim5412$ cm^{-1} in the EPR analysis (Fig. S1a). The highest occupied molecular orbital (HOMO) shape suggests the low-level orbital of e_g^* of the Cu coordination compound was $d_{x^2-y^2}$ (Fig. S1b).

Polysaccharides are one of the main compositions for EPS and sludge microorganisms, and the glucose with plenty of hydroxyl groups is one of the main units of polysaccharides[31,32]. The optimized structure of distorted octahedra with Cu center contains four short equatorial bonds and two elongated axial bonds (Fig. 5a), and the angle of distortion is shown in Fig. 5b. The position of octahedrally coordinate around the Cu did not change significantly in the energy minimization. The detailed bond distances and angles of the Cu complexing structure calculated by DFT fitted well with the experimental data (Table 2). The critical bond angles demonstrate that the Cu complex had distorted coordinated octahedral structure, which was comprised of four short equatorial O atoms connected with C from glucose and two elongated axial O with H from H_2O. Four short equatorial O atoms from hydroxyl groups of two glucose molecules form two hexatomic rings with Cu as shown in Fig. 5b. The Cu(II) center is connected with two glucose molecules and two H_2O to form hexa-coordinated Cu-sludge complex. The distances of Cu-O5 and Cu-O6 were calculated to be 2.29 Å and 2.28 Å, respectively, which were slightly smaller than those obtained from the XAFS spectra (2.40–2.50 Å) and close to the reported $Cu\text{-}O_{ax}$ distance 2.29–2.41 Å. The glucose molecule was bound end-on to the Cu(II) center with Cu–O distances of horizontal plane in a range of 2.05–2.10 Å. This agreed with the experimental $Cu\text{-}O_{eq}$ from the XAFS analysis, implying the computational models used for DFT calculation was reasonable. In this case, the Cu complex shown in Fig. 5 was considered to be the most stable one with the lowest energy.

Implications of this work. Though the macroscopic interactions between metals and microorganisms have been extensively studied, it is still of great significance to explore such a complexation from a microscopic viewpoint and to observe the microstructure. In the present work, a multi-technique approach was used to probe the complexing characteristics between Cu(II) and microbial cells, and it was proven to be a powerful tool to elucidate such an interaction between heavy metals and activated sludge microorganisms. XAFS and EPR could provide the local structure and geometrical information of Cu. Meanwhile, DFT calculations are able to describe the structural geometry of the Cu complex. Spectroscopic studies confirmed Cu complexation via the formation of inner-sphere surface complexes as the major mechanism of biosorption, and the DFT method was used to calculate the most stable Cu complex structures. These results could be useful for better
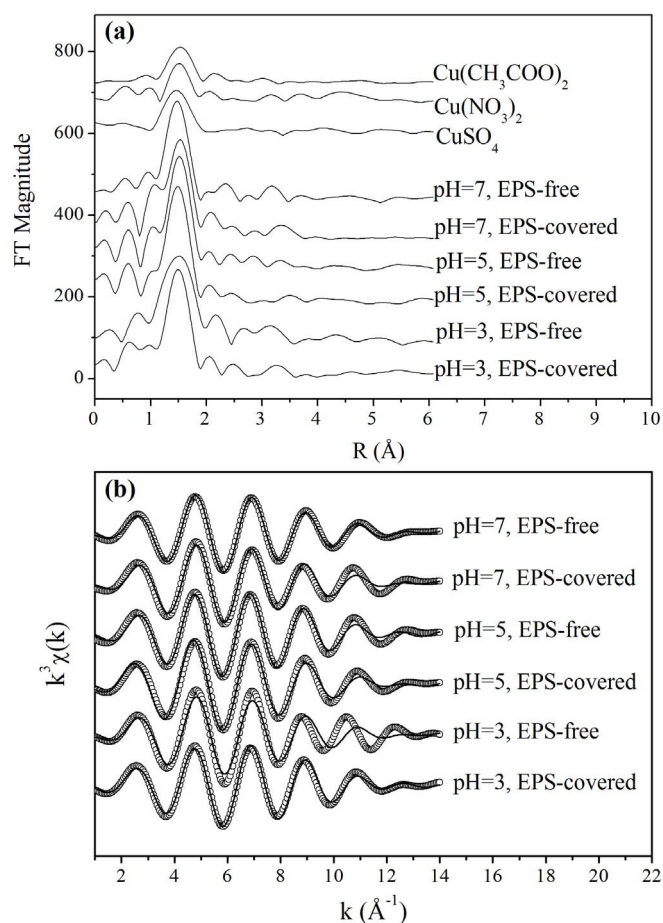

Figure 4 | (a) RSF obtained by Fourier transformation of the EXAFS spectrum; and (b) first-shell fit of the EXAFS function of the Cu(II)-activated sludge complex, nonlinear least-squares fits (solid lines) and experimental data (open circles).

Table 1 | Levenberg-Marquardt Fitting of Cu K-edge Bulk XAS Analysis

		First shell (Cu-O$_{eq}$)					Second shell (Cu-O$_{ax}$)	
pH	Cu sample	R (Å)	CN	E$_0$ shift (eV)	σ²(Å²) × 10^{-3}	relative error (%)	R (Å)	CN
3.0	EPS-covered	1.93 ± 0.01	4.0 ± 0.3	3.4 ± 0.9	6.9 ± 0.5	5.7	2.40 ± 0.20	1.5 ± 0.9
3.0	EPS-free	1.94 ± 0.01	4.0 ± 0.5	6.3 ± 1.4	7.9 ± 0.8	9.5	2.43 ± 0.50	1.7 ± 0.5
5.0	EPS-covered	1.94 ± 0.01	4.0 ± 0.2	5.8 ± 0.6	6.6 ± 0.4	3.3	2.43 ± 0.10	1.7 ± 0.6
5.0	EPS-free	1.95 ± 0.02	4.0 ± 0.3	5.1 ± 1.0	6.9 ± 0.6	5.3	2.50 ± 0.10	1.8 ± 0.6
7.0	EPS-covered	1.95 ± 0.01	4.0 ± 0.4	7.8 ± 1.1	7.9 ± 0.7	7.3	2.47 ± 0.30	1.7 ± 0.7
7.0	EPS-free	1.94 ± 0.01	4.0 ± 0.3	5.0 ± 0.9	7.6 ± 0.3	2.8	2.41 ± 0.20	1.6 ± 0.7

R: Interatomic distance (Å); CN: Coordination number.
E$_0$ shift: edge energy (eV); σ²: Debye-Waller factor (Å²).

understanding the speciation, immobilization, transport, and bioavailability of heavy metals in biological wastewater treatment plants, and might also be beneficial for exploring the geochemical cycle of metals in natural waters and soils.

Conclusions

The microscopic-level complexing between heavy metal Cu(II) and activated sludge has been studied. Spectroscopic results indicate that Cu complexed with activated sludge via the formation of inner-sphere surface complexes of octahedral coordination with tetragonal distortion of axial elongation, containing four short equatorial bonds with a mean Cu-O$_{eq}$ bond distance of 1.95 Å and two elongated axial bonds with a Cu-O$_{ax}$ bond distance of 2.43 Å. DFT calculation was able to explain the structural geometry of the Cu complex, and fitted well with the experimental results. These results would be useful for understanding the mechanism of the fate and species of Cu(II) in biological wastewater treatment plants.

Methods

EPS extraction from activated sludge and Cu(II) adsorption tests. The activated sludge was harvested from a laboratory-scale sequencing batch reactor fed with a synthetic wastewater, which the composition was: CH$_3$COONa, 640 mg L^{-1}; NH$_4$Cl, 95 mg L^{-1}; KH$_2$PO$_4$, 22.5 mg L^{-1}; CaCl$_2$, 11.5 mg L^{-1}; MgSO$_4$, 12 mg L^{-1} and 10 mL of trace element solution. The C: N: P ratio was 100 : 5 : 1. The reactor was operated

Figure 5 | DFT optimized results: (a) Local structures of Cu complex; and (b) Top view to show the bond angle.

sequentially in 6 h cycles, with 7 min of substrate filling, 342 min of aeration, 2 min of settling and 3 min of effluent withdraw. The sludge concentration was 3.6 g/L, and the ratio of volatile suspended solids (VSS) to suspended solids (SS) was 0.82, implying the high microorganism contents in the sludge. Before experiments, the sludge microorganisms were washed by distilled water for three times to remove the residual substrate and metabolic products. The EPS were extracted using the cation exchange resin (CER) technique as described previously[33]. Briefly, the activated sludge sample, washed twice with 50 mM NaCl solution, was stirred for 12 h at 200 rpm and 4°C after the CER addition (60 g/g SS). Subsequently, the solutions were centrifuged to remove CER and remaining sludge components. The supernatants were then filtered through 0.45 µm cellulose acetate membranes and used as the EPS fraction.

The process of Cu(II) biosorption was conducted using 50 mL shaking flasks. The detailed information about characterization of the Cu(II) biosorption onto sludge has been given in the Supplementary Information. The maximum Cu retention capacity of the activated sludge at pH 5.0 was calculated to be 25.7 mg/g through Langmuir adsorption isotherm model (Fig. S2). The microstructure of Cu(II) complexing with the functional groups in activated sludge were explored using XAFS and EPR techniques, and high content of complexed Cu(II) on sludge would be beneficial for the accuracy of XAFS and EPR analysis. Herein, Cu(II) concentration at 64 mg/L and 2.08 g of activated sludge were added to the flasks and mixed. The ionic strength was adjusted to 50 mM NaCl. The pH was adjusted to 3.0, 5.0 and 7.0. After 12 h of equilibrium, the sludge after complexing with Cu(II) was carefully washed twice by 50 mM NaCl solution to remove the remaining free Cu(II) ions, and then used for XAFS and EPR analysis. The sludge after EPS extraction was also used for comparison.

Potentiometric titration. The surface functional groups of activated sludge were determined with the potentiometric titration. The sludge resuspended in 40 mL solution (6.0 g-dry weight/L) was titrated using a DL 50 Automatic titrator (Mettler Toledo Co., Switzerland) with a pH electrode of 0.001 precision. The titration was conducted under nitrogen gas conditions at 25°C. The solution ionic strength was adjusted to 0.01 mol/L. The initial pH was adjusted to 3.0 by 1 mol/L HCl, and was titrated by 0.1 mol/L NaOH with 10 µL increments until pH 11.0 was reached. The titration data obtained were analyzed using the PROTOFIT 2.1 software[34].

XAFS measurements and analysis. The Cu K-edge XAFS spectra of Cu(II) sorbed on the activated sludge were measured at the U7C beamline of the National Synchrotron Radiation Laboratory (NSRL), Hefei, China. The XAFS signals were collected in a fluorescence mode with a seven-element high-purity Ge solid detector. The electron beam energy was 0.8 GeV and the maximum stored current was 300 mA. A double crystal Si (1 1 1) monochromator was used. Energy calibration was monitored using a Cu metallic foil with the first inflection of the absorption edge set to 8979 eV. The spectra were recorded in the energy range of 8779–9774 eV covering the copper K-edge (≈8979 eV) with intervals of 0.5 eV for XANES and 2 eV for EXAFS. An integration time of 5.0 s per point was used in both cases. The obtained data of all the standards and samples in three scans were averaged to improve the signal to noise ratios (S/N), which was more than 10³ under the experimental conditions. The raw data analysis was performed by using the NSRL-XAFS 3.0 software package according to the standard data analysis procedures[35].

EPR measurement. The EPR spectra of Cu(II) complex with activated sludge before EPS extraction at pH = 5.0 were measured using an EMX spectrometer (Bruker Co., Germany) at 40 K and 298 K, which was operated at X-band frequency (9.72 GHz) with a 100 kHz modulation frequency. Sample pretreatments for the EPR measurement were consistent with those for the XAFS measurement. All measurements were repeated four times, and a gradient cooling method was applied: a) solid ethanol (190 K); b) liquid nitrogen (77 K); and c) liquid helium (40 K), to avoid the breaking of the EPR sample tubes. The EPR spectra were recorded at a microwave power of 2 mW and modulation amplitude of 5.0 G.

DFT calculation. All the calculations were completed using the DMol³ module[36,37] of the Materials Studio Program. The minimum-energy geometry structures of the Cu complex were determined by an all-electron method within the Perdew-Wang
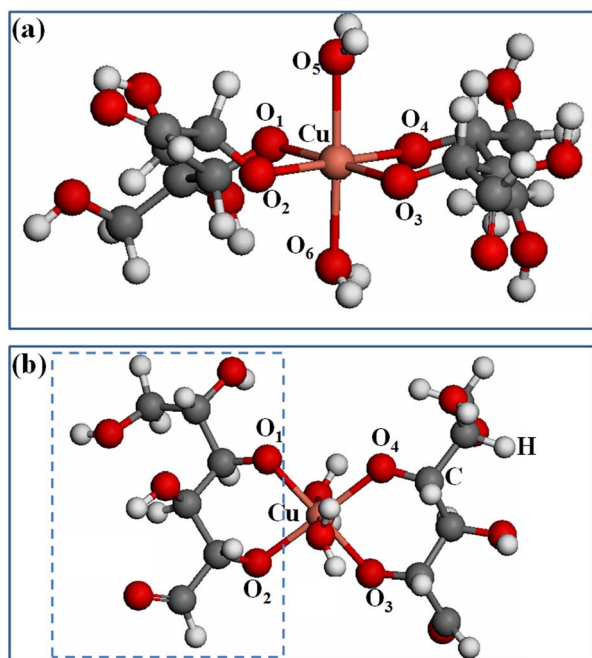
Table 2 | Selected Bond Distances (Å) and Angles (°) of the Cu Complexing Structure (Figure 5) Calculated by DFT Method

	Geometry structure	DFT optimized structure	Cu K-edge EXAFS experiment
Bond	Cu-O1	2.086	1.93~1.95
	Cu-O2	2.103	
	Cu-O3	2.056	
	Cu-O4	2.064	
	Cu-O5	2.287	2.29~2.50
	Cu-O6	2.281	
Angle	O1-Cu-O6	89.372	distorted octahedral structure
	O2-Cu-O6	89.832	
	O3-Cu-O5	92.021	
	O4-Cu-O5	91.109	

91 (PW91) form of generalized gradient approximation (GGA)[38,39] for the exchange-correlation term. The double precision numerical basis sets including p polarization (DNP) were adopted. A spin-polarized scheme was employed to deal with the open-shell systems. The energy in each geometry optimization cycle was converged to within 2×10^{-5} Hartree with a maximum displacement and force of 5×10^{-3} Å and 4×10^{-3} Hartree/Å, respectively.

The computational models of the active sites were constructed from carboxyl, hydroxyl and glucose units, which were one of the main compositions for EPS and sludge microorganisms[31]. Combined with XAFS and EPR results, geometry optimization of Cu complex was performed with frequent updates of the force constants in order to stay as close as possible to the lowest energy pathway. The complex was regarded to reach a most stable structure when the energy came to the lowest horizontal line. Furthermore, the splitting result of orbital energy level and the analysis of orbital elements could also be obtained.

1. Vaiopoulou, E. & Gikas, P. Effects of chromium on activated sludge and on the performance of wastewater treatment plants: A review. *Water Res.* **46**, 549–570 (2012).
2. Park, C. & Novak, J. T. Characterization of activated sludge exocellular polymers using several cation-associated extraction methods. *Water Res.* **41**, 1679–1688 (2007).
3. Tong, M., Long, G., Jiang, X. & Kim, H. N. Contribution of extracellular polymeric substances on representative Gram Negative and Gram Positive bacterial deposition in porous media. *Environ. Sci. Technol.* **44**, 2393–2399 (2010).
4. Das, S. K., Ghosh, P., Ghosh, I. & Guha, A. K. Adsorption of rhodamine B on *Rhizopus oryzae*: Role of functional groups and cell wall components. *Colloid Surf. B.* **65**, 30–34 (2008).
5. Ueshima, M. *et al.* Cd adsorption onto *Pseudomonas putida* in the presence and absence of extracellular polymeric substances. *Geochim. Cosmochim. Acta.* **72**, 5885–5895 (2008).
6. Fang, L. C. *et al.* Role of extracellular polymeric substances in Cu(II) adsorption on *Bacillus subtilis* and *Pseudomonas putida*. *Bioresour. Technol.* **102**, 1137–1141 (2011).
7. Benaïssa, H. & Elouchdi, M. A. Biosorption of copper (II) ions from synthetic aqueous solutions by drying bed activated sludge. *J. Hazard. Mater.* **194**, 69–78 (2011).
8. Laurent, J., Casellas, M., Carrère, H. & Dagot, C. Effects of thermal hydrolysis on activated sludge solubilization, surface properties and heavy metals biosorption. *Chem. Eng. J.* **166**, 841–849 (2011).
9. Sag, Y., Tatar, B. & Kutsal, T. Biosorption of Pb(II) and Cu(II) by activated sludge in batch and continuous-flow stirred reactors. *Bioresour. Technol.* **87**, 27–33 (2003).
10. Ha, J., Gelabert, A., Spormann, A. M. & Brown, G. E. Role of extracellular polymeric substances in metal ion complexation on *Shewanella oneidensis*: Batch uptake, thermodynamic modeling, ATR-FTIR and EXAFS study. *Geochim. Cosmochim. Acta.* **74**, 1–15 (2010).
11. Drzewiecka, A. *et al.* Synthesis and structural studies of novel Cu(II) complexes with hydroxy derivatives of benzo[b]furan and coumarin. *Polyhedron* **43**, 71–80 (2012).
12. Wang, X. Y., Deng, X. T. & Wang, C. G. Bis (acetato-*k*²O,O′) diaquacopper(II). *Acta Crystallogr. Sect. E.-Struct Rep.* **62**, M3578–M3579 (2006).
13. Adamescu, A., Hamilton, I. P. & Al-Abadleh, H. A. Thermodynamics of dimethylarsinic acid and arsenate interactions with hydrated iron-(oxyhydr)oxide clusters: DFT calculations. *Environ. Sci. Technol.* **45**, 10438–10444 (2011).
14. He, G. Z., Pan, G., Zhang, M. Y. & Waychunas, G. A. Coordination structure of adsorbed Zn(II) at water-TiO₂ interfaces. *Environ. Sci. Technol.* **45**, 1873–1879 (2011).
15. Jin, X., Yan, Y., Shi, W. & Bi, S. Density functional theory studies on the structures and water-exchange reactions of aqueous Al(III)-oxalate complexes. *Environ. Sci. Technol.* **45**, 10082–10090 (2011).
16. Braissant, O. *et al.* Exopolymeric substances of sulfate-reducing bacteria: Interactions with calcium at alkaline pH and implication for formation of carbonate minerals. *Geobiol.* **5**, 401–411 (2007).
17. Laurent, J., Pierra, M., Casellas, M. & Dagot, C. Fate of cadmium in activated sludge after changing its physico-chemical properties by thermal treatment. *Chemosphere.* **77**, 771–777 (2009).
18. Lee, S. M. & Davis, A. P. Removal of Cu(II) and Cd(II) from aqueous solution by seafood processing waste sludge. *Water Res.* **35**, 534–540 (2001).
19. Liu, H. & Fang, H. H. P. Characterization of electrostatic binding sites of extracellular polymers by linear programming analysis of titration data. *Biotechnol. Bioeng.* **80**, 806–811 (2002).
20. Bahranowski, K., Dula, R., Labanowska, M. & Serwicka, E. M. ESR study of Cu centers supported on Al-, Ti-, and Zr-pillared montmorillonite clays. *Appl. Spectrosc.* **50**, 1439–1445 (1996).
21. Motschi, H. Correlation of EPR-parameters with thermodynamic stability constants for copper(II) complexes - Cu(II) electron paramagnetic resonance as a probe for the surface complexation at the water/oxide interface. *Colloids Surf.* **9**, 333–347 (1984).
22. Flogeac, K., Guillon, E. & Aplincourt, M. Surface complexation of copper(II) on soil particles: EPR and XAFS studies. *Environ. Sci. Technol.* **38**, 3098–3103 (2004).
23. Frenkel, A. I., Korshin, G. V. & Ankudinov, A. L. XANES study of Cu²⁺-binding sites in aquatic humic substances. *Environ. Sci. Technol.* **34**, 2138–2142 (2000).
24. Strawn, D. G. & Baker, L. L. Speciation of Cu in a contaminated agricultural soil measured by XAFS, μ-XAFS and μ-XRF. *Environ. Sci. Technol.* **42**, 37–42 (2008).
25. Furnare, L. J., Vailionis, A. & Strawn, D. G. Polarized XANES and EXAFS spectroscopic investigation into copper(II) complexes on vermiculite. *Geochim. Cosmochim. Acta.* **69**, 5219–5231 (2005).
26. Choy, J. H., Yoon, J. B. & Jung, H. Polarization-dependent X-ray absorption spectroscopic study of [Cu(cyclam)](2+)-intercalated saponite. *J. Phys. Chem. B.* **106**, 11120–11126 (2002).
27. Karlsson, T., Persson, P. & Skyllberg, U. Complexation of copper(II) in organic soils and in dissolved organic matter - EXAFS evidence for chelate ring structures. *Environ. Sci. Technol.* **40**, 2623–2628 (2006).
28. Hsiao, M. C., Wang, H. P. & Yang, Y. W. EXAFS and XANES studies of copper in a solidified fly ash. *Environ. Sci. Technol.* **35**, 2532–2535 (2001).
29. Korshin, G. V., Frenkel, A. I. & Stern, E. A. EXAFS study of the inner shell structure in copper(II) complexes with humic substances. *Environ. Sci. Technol.* **32**, 2699–2705 (1998).
30. Scheinost, A. C., Abend, S., Pandya, K. I. & Sparks, D. L. Kinetic controls on Cu and Pb sorption by ferrihydrite. *Environ. Sci. Technol.* **35**, 1090–1096 (2001).
31. Wang, Z., Choi, O. & Seo, Y. Relative contribution of biomolecules in bacterial extracellular polymeric substances to disinfection byproduct formation. *Environ. Sci. Technol.* **47**, 9764–9773 (2013).
32. Dignac, M. F. *et al.* Fate of wastewater organic pollution during activated sludge treatment: nature of residual organic matter. *Water Res.* **34**, 4185–4194 (2000).
33. Sheng, G. P., Zhang, M. L. & Yu, H. Q. Characterization of adsorption properties of extracellular polymeric substances (EPS) extracted from sludge. *Colloids Surf. B-Biointerfaces* **62**, 83–90 (2008).
34. Turner, B. F. & Fein, J. B. Protofit: A program for determining surface protonation constants from titration data. *Comput. Geosci.* **32**, 1344–1356 (2006).
35. Sayers, D. E. & Bunker, B. A. Data analysis. *X-ray Absorption, Principles, Applications, Techniques of EXAFS, SEXAFS and XANES* [Koningsberger, D.C., Prins, R. (eds.)] [211–253] (Wiley, New York, 1998).
36. Delley, B. Fast calculation of electrostatics in crystals and large molecules. *J. Phys. Chem.* **100**, 6107–6110 (1996).
37. Delley, B. From molecules to solids with the DMol(3) approach. *J. Phys. Chem.* **113**, 7756–7764 (2000).
38. Perdew, J. P. *et al.* Atoms, molecules, solids and surfaces: Applications of the generalized gradient approximation for exchange and correlation. *Phys. Rev. B.* **46**, 6671–6687 (1992).

39. Perdew, J. P. & Wang, Y. Accurate and simple analytic representation of the electron-gas correlation energy. *Phys. Rev. B. Condens. Matter.* **45**, 13244–13249 (1992).

Acknowledgments

Author contributions

H.W.L. and J.J.C. carried out the experiments, analyzed the data, and wrote the paper; G.P.S. designed the experiments, analyzed the data, and wrote the paper; J.H.S. designed the EPR experiments and analyzed EPR data, and S.Q.W. analyzed the XAFS data; H.Q.Y. analyzed the data and wrote the paper.

Additional information

Supplementary information accompanies this paper at http://www.nature.com/scientificreports

Competing financial interests: The authors declare no competing financial interests.

How to cite this article: Luo, H.-W. *et al.* Experimental and Theoretical Approaches for the Surface Interaction between Copper and Activated Sludge Microorganisms at Molecular Scale. *Sci. Rep.* **4**, 7078; DOI:10.1038/srep07078 (2014).